

# A distributed Gaussian approach to the vibrational dynamics of Ar-benzene

J. Faeder<sup>a)</sup>

Department of Chemistry and Biochemistry, University of Colorado, and Joint Institute for Laboratory Astrophysics, University of Colorado and National Institute of Standards and Technology, Boulder, Colorado 80309-0440

(Received 14 June 1993; accepted 10 August 1993)

A method for calculating the vibrational eigenstates of van der Waals clusters is presented and applied to argon-benzene. The method employs the linear variational principle with a nonorthogonal basis set of Gaussian functions in both the stretching and bending coordinates. These localized functions allow greater flexibility than the standard spherical harmonics or Wigner  $D$  functions and should be more efficient when the motion is confined to specific regions of the potential energy surface. Calculations are performed on several potential surfaces including two recent fits to a previously published *ab initio* calculation. Accurate results with rapid convergence are obtained here for the states of zero total angular momentum ( $J=0$ ). The results agree with calculations recently performed on the same potential surfaces by a different method [J. Chem. Phys. **98**, 5327 (1993)] and suggest a reassignment of the experimentally observed bands. An extension of the basis set to nonzero  $J$  is presented in the Appendix.

## I. INTRODUCTION

High-resolution spectroscopy of intermolecular vibrations in van der Waals (vdW) complexes provides a sensitive probe of intermolecular forces. The rapidly accumulating wealth of spectroscopic data has created a demand for efficient and adaptable means to calculate the vibrational states of weakly bound complexes from trial potential energy surfaces. The development of more efficient computational methods along with the widespread availability of high-speed computers has enabled accurate determination of the multi-dimensional intermolecular potentials for several atom-molecule systems.<sup>1-3</sup> For systems of more than two dimensions, however, the procedure remains difficult and expensive. There is a continuing need for computational methods that are both easy to implement and scale well with increasing dimension.

Weakly bound systems pose a particular challenge because the standard "normal modes" are often strongly coupled, and thus provide an inadequate description of the vibrational motion. In many vdW complexes, the bending motion of the monomers is more accurately described as free internal rotation, in which the angular momentum of the monomers is nearly conserved. This suggests expanding the solution in a basis set of rotational eigenfunctions, spherical harmonics or Wigner  $D$  functions depending on the dimension of the problem. Delocalized functions are appropriate for complexes near the free-rotor limit, but become inefficient when the angular motion is hindered.

Consider the case of an atom-molecule complex. As the center-of-mass separation decreases, the barrier to rotation of the molecule about its center-of-mass increases. When the radius of the molecule is comparable to or larger than the equilibrium separation, large regions of the angu-

lar configuration space may become inaccessible due to the strong nuclear repulsions. Direct product basis sets where the angular functions cover the entire angular space will have flux in these regions, and a large number of angular basis functions will be necessary to localize the eigenstates on the accessible region of the potential. Calculations based on these basis sets will thus converge very slowly. The problem becomes particularly intractable for rare-gas-aromatic complexes.<sup>4,5</sup> The close-coupling,<sup>6</sup> collocation,<sup>7,8</sup> and standard variational<sup>4,9</sup> approaches all explicitly rely on expansions in the angular eigenfunctions. Until recently,<sup>10</sup> implementations of the discrete-variable representation (DVR) method<sup>11</sup> have also relied implicitly on such angular expansions.

To avoid the problems associated with spherical function basis sets, Brocks and van Koeven<sup>5</sup> have derived an exact body-fixed Hamiltonian in Cartesian coordinates and have performed variational calculations using localized harmonic oscillator basis sets with good results. This method has been employed in the recent calculations of van der Avoird.<sup>12</sup> Mandziuk and Bačić have also used the Cartesian Hamiltonian of Brocks and van Koeven in their recent three-dimensional DVR calculations on Ar-naphthalene.<sup>10</sup> The DVR<sup>13</sup> in each dimension is a pointwise representation associated with a particular set of orthogonal basis functions, which are harmonic oscillator functions in this case. The three-dimensional DVR is the direct product of three one-dimensional DVR's. The kinetic energy matrix in the DVR is given by transforming the kinetic energy matrix in the harmonic oscillator basis using the DVR transformation,<sup>13</sup> while the potential energy matrix is approximately given as a diagonal matrix of the potential evaluated at the DVR points. The major advantages of the DVR are that it eliminates the need for multidimensional integration to evaluate the potential energy matrix and that it gives rise to a straightforward procedure of truncating the Hamiltonian matrix to reduce the

<sup>a)</sup>Supported under a National Science Foundation Graduate Research Fellowship.

size of the matrix diagonalization that must be performed.<sup>11</sup> DVR points in the highly repulsive regions of the potential may also be removed from the basis.<sup>11</sup> However, the DVR also inherits the weaknesses of the basis functions from which it is defined. A DVR method based on angular momentum functions will be more efficient than a standard variational approach, but will still encounter difficulties when applied to problems where these basis functions are less appropriate. Single-center basis sets, such as the harmonic-oscillator functions, become inefficient when there are multiple potential minima, such as occur in larger clusters or in clusters of high symmetry. A basic limitation of the DVR is that the pointwise representation must be associated with a particular set of orthogonal functions and no single set of orthogonal functions will be well-suited to the full range of problems.

Multidimensional Gaussians,<sup>14</sup> i.e., functions that are a product of a single Gaussian function in each coordinate, provide a more flexible approach. A major advantage of multidimensional Gaussian basis sets is their simplicity. They are localized in the multidimensional space, and an efficient nondirect-product basis set may be constructed for a given problem simply by placing the Gaussian centers in regions of the potential energy surface where wave function amplitude is expected for the energies of interest. These regions need not be contiguous and the density of basis functions may be tailored to the shape of the potential surface. The matrix elements are either analytical or may be evaluated by simple quadrature schemes which exploit the various properties of Gaussian functions.<sup>14</sup> In addition, it might be possible to use the collocation method, which allows the construction of a more general but more approximate pointwise representation than the DVR, to avoid numerical integration.<sup>7</sup> Collocation with the Gaussian basis set and the curvilinear Hamiltonian used here is not possible because of singularities that arise at  $\theta=0$ . A multidimensional Gaussian basis set for which collocation would be possible could be constructed for the Cartesian Hamiltonian of Brocks and van Koeven.

For the case of Ar-CO<sub>2</sub> Peet<sup>15</sup> has shown that a localized basis set of two-dimensional Gaussians can yield a 35%–40% reduction in basis set size over a basis of monomer rotational functions and radial Gaussians. Rare-gas-aromatic complexes provide a good proving ground for the extension of localized basis-set methods. The bending motion in these complexes is large enough to invalidate small amplitude approximations, but is still confined to a relatively small region of the configuration space (e.g.  $\sim 10^\circ$  in Ar-benzene). If high accuracy is desired, multidimensional calculations must be carried out. These systems possess an additional internal degree of freedom over the atom-linear molecule complexes, and require both modification and extension of the angular Gaussian basis set used by Peet. As the angular momentum in this additional coordinate is nearly conserved, however, Gaussians are used only in the original two dimensions. One apparent disadvantage of the Gaussian basis in curvilinear coordinates is that the rotational boundary conditions must be explicitly worked out and imposed on the basis functions. This is

shown to be a straightforward process. An appropriately modified basis set, described below, provides a highly efficient and easy-to-implement method for treating the vibrational dynamics of rare-gas-aromatic complexes. Furthermore, the extension described here should generalize to the treatment of molecule-molecule complexes in internal angular coordinates using distributed Gaussian basis sets.

Argon-benzene is singled out here because of the availability of both theoretical and spectroscopic data, and because previous calculations of the vdW vibrations provide a basis of comparison to other methods. The equilibrium configuration of the complex is known from both rotational<sup>16</sup> and electronic<sup>17–19</sup> spectroscopy to have  $C_{6v}$  symmetry. *Ab initio* studies have also predicted this geometry for the complex.<sup>20</sup> Attempts to assign the small number of observed vibrational bands on the basis of normal mode calculations have been unsuccessful.<sup>17,21</sup> These failures resulted in part from lack of an accurate potential energy surface for the complex, and in part because the one-dimensional calculations present an inaccurate and misleading picture of the dynamics. Brocks and Huygen's fully three-dimensional calculations on an empirical potential<sup>4</sup> showed that there is strong anharmonic coupling between the bending overtone and the stretch fundamental characteristic of a Fermi resonance. Anharmonic bend-stretch coupling also seems to account for anomalies in a number of other rare-gas-aromatic spectra<sup>22</sup> and should provide a stringent test for the validity of a given potential. This coupling is examined in detail here through a comparison of the uncoupled (adiabatic) and coupled states calculated using a localized basis.

While this work was in progress, van der Avoird<sup>12</sup> has published calculations on the same two *ab initio* fit surfaces<sup>23</sup> employed here. His results are in excellent agreement with those reported here and confirm the correctness of both methods. Based on a similar analysis to that presented below, he also proposes the same reassignment of the experimental spectrum. This reassignment has in fact been carried out and shown to be correct.<sup>24</sup>

## II. METHOD

### A. Coordinate system

The coordinates used here have been previously derived by Brocks *et al.*<sup>25</sup> and have been widely used for calculations on atom-molecule complexes. The body-fixed frame is defined by the vector  $R$  from the molecule center-of-mass to the atomic center. The two Euler angles  $\alpha$  and  $\beta$  define the orientation of this vector with respect to a space-fixed coordinate system. The use of two rather than three Euler angles for this coordinate embedding has been shown to result in a clearer form of the Hamiltonian.<sup>25</sup> Three more Euler angles,  $\theta$ ,  $\phi$ , and  $\chi$ , specify the orientation of the molecule-fixed axes with respect to the body-fixed frame. To make use of the molecular symmetry, the molecule-fixed  $z$ -axis is defined to be coincident with the  $C_6$  axis of the benzene, with the origin located at the benzene center-of-mass, as shown in Fig. 1. The Cartesian coordinates of the argon atom in this molecule-fixed sys-

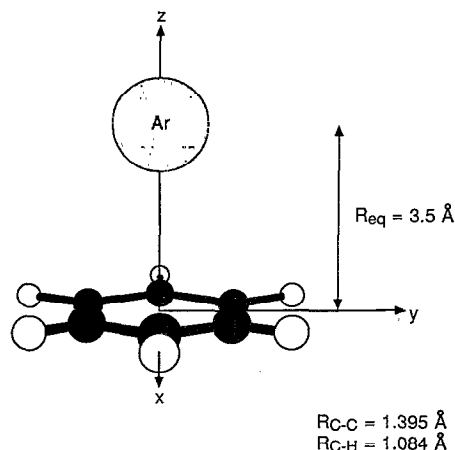


FIG. 1. Body-fixed coordinate system of the Ar–benzene complex. The coordinates are of the argon atom moving around the benzene molecule fixed at the origin in the  $x$ - $y$  plane. The center-of-mass separation  $R$  and the two Euler angles  $\theta$  and  $\chi$  are then the standard spherical polar coordinates for the Cartesian frame.

tem are then given in the standard way by the spherical polar coordinates  $R$ ,  $\theta$ , and  $\chi$ . The interaction potential depends only on these three coordinates, but not on the remaining Euler angle  $\phi$ , which defines a rotation of the molecular axis system about  $R$ . The angles  $\alpha$ ,  $\beta$ , and  $\phi$  are thus referred to as “rotational” coordinates, while the angles  $\theta$  and  $\chi$  are referred to as “vibrational.” This is an important distinction, since we wish to use a localized basis only for the vibrational coordinates, in which the motion may be hindered. The angular momentum functions will remain a good basis for the rotational motions. Although it is convenient to visualize the benzene as fixed, it is important to keep in mind that the actual bending motion is librational in a space-fixed frame.

## B. Hamiltonian

The Hamiltonian for an atom–molecule interaction in body-fixed coordinates can be written as<sup>25</sup>

$$H = H_{\text{int}} + H_{\text{mol}}, \quad (1)$$

where  $H_{\text{mol}}$  is the isolated molecular Hamiltonian and the interaction term is

$$H_{\text{int}} = -\frac{\hbar^2}{2\mu R} \frac{\partial^2}{\partial R^2} R + \frac{\hbar^2}{2\mu R^2} (\hat{J}^2 - 2\hat{\mathbf{j}} \cdot \hat{\mathbf{J}} + \hat{j}^2) + V_{\text{int}}. \quad (2)$$

$\hat{\mathbf{J}}$  is the total angular momentum operator of the complex,  $\hat{\mathbf{j}}$  is the angular momentum operator of the benzene monomer,  $R$  is the center-of-mass separation, and  $\mu$  is the reduced mass of the complex. The first two terms are just the radial and rotational kinetic energies of the complex. Since the intramolecular vibrations of the benzene are much faster than the intermolecular motions of the complex, the interaction potential,  $V_{\text{int}}$ , may be written as a function of the intermolecular coordinates  $R$ ,  $\theta$ , and  $\chi$  for a given vibronic state of the benzene monomer. This is analogous

to the Born–Oppenheimer approximation for nuclear motion. Benzene is a symmetric top, so the molecular Hamiltonian may be written as

$$H_{\text{benz}} = A\hat{j}^2 - (A-C)\hat{j}_z^2 + E^{\text{vib,ele}}, \quad (3)$$

where  $\hat{j}_z$  is the projection of the monomer angular momentum on the monomer  $z$  axis,  $A$  and  $C$  are the vibrationally averaged symmetric top rotation constants, and we have simply added the energy of the vibrational and electronic state of benzene. Both the interaction potential and the averaged rotation constants depend on the vibronic state of the benzene. Note that the Hamiltonian for any atom-rigid-top complex may be obtained simply by substituting the appropriate interaction potential and the appropriate rotational Hamiltonian into the above expressions.

For simplicity, we consider here only the case of  $J=0$ . The nonzero  $J$  basis set and Hamiltonian are discussed in the Appendix. It is important to note that symmetric or asymmetric top complexes, unlike linear complexes, may have  $J=0$  states with nonzero vibrational angular momentum. This is because overall rotation about the intermolecular axis may cancel the angular momentum contribution due to degenerate vibrations in the symmetric top case, but not in the linear case. Thus, every vdW vibrational state in a nonlinear complex has a  $J=0$  component, the spectroscopic band origin. The more complicated calculations at nonzero  $J$  are needed to determine the exact rotational structure and the Coriolis interactions.

The Hamiltonian for  $J=0$  becomes

$$H = -\frac{\hbar^2}{2\mu R} \frac{\partial^2}{\partial R^2} R + \left( \frac{\hbar^2}{2\mu R^2} + A \right) \hat{j}^2 - (A-C)\hat{j}_z^2 + V(R, \theta, \chi) + E^{\text{vib,ele}}. \quad (4)$$

It is now clear that  $\hat{j}_z$  commutes with the kinetic part of the Hamiltonian for an atom–symmetric top complex. If the azimuthal dependence of the interaction potential is weak, as it is for Ar–benzene, one would expect the azimuthal angular momentum quantum number,  $k$ , to be nearly conserved. This fact will be exploited in the construction of the angular basis. Using the coordinate representation of the body-fixed angular momentum operator  $\hat{\mathbf{j}}$ , we may write the full Hamiltonian in terms of the body-fixed spherical polar coordinates

$$H = -\frac{\hbar^2}{2\mu R} \frac{\partial^2}{\partial R^2} R - \left[ \frac{\hbar^2}{2\mu R^2} + A \right] \left( \frac{1}{\sin^2 \theta} \frac{\partial^2}{\partial \chi^2} + \frac{1}{\sin \theta} \frac{\partial}{\partial \theta} \left( \sin \theta \frac{\partial}{\partial \theta} \right) \right) + (A-C) \frac{\partial^2}{\partial \chi^2} + V(R, \theta, \chi), \quad (5)$$

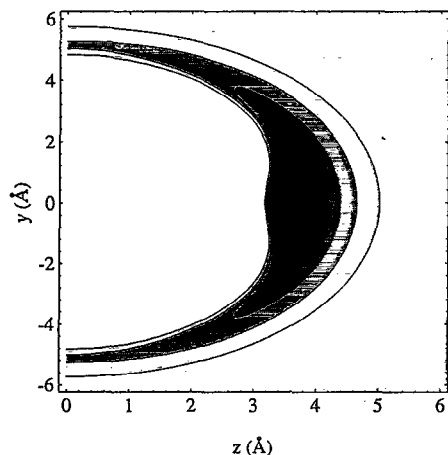


FIG. 2. Contour plot of the *ab initio* argon–benzene interaction potential of Ref. 23 (global fit A). The darkest contour is at  $-360\text{ cm}^{-1}$ , the lightest is at  $-110\text{ cm}^{-1}$ , and the contours are spaced  $50\text{ cm}^{-1}$  apart.

where the first three terms comprise the kinetic energy operator of the complex.

### C. Interaction potential

Calculations were performed on both an empirical potential surface employed in several previous works,<sup>4</sup> and on a recently published *ab initio* surface.<sup>23</sup> For comparison and to test the effects of anharmonicity, calculations were performed on two separate fits to the *ab initio* potential points. The global fit from Ref. 23 provides a representation of the potential over the entire surface, while the Morse fit is more accurate near the region of the minimum. The empirical and global fit potentials have the atom–atom pairwise form

$$V(\mathbf{R}) = \sum_{i=1}^6 [v_C(r_{Ar-C_i}) + v_H(r_{Ar-H_i})], \quad (6)$$

where  $v_C$  and  $v_H$  are functions of the argon–carbon and argon–hydrogen internuclear separations, respectively. The Morse fit potential has the form

$$V(x, y, z) = k_{zz}w^2 + k_{xx}(x^2 + y^2) + k_{xxz}w(x^2 + y^2) - D_e, \quad (7)$$

where  $D_e$  is the potential well depth,  $z_e$  is the equilibrium center-of-mass separation and

$$w = 1 - e^{-a(z-z_e)}. \quad (8)$$

The first three terms correspond to a Morse potential in the  $z$  coordinate, a harmonic restoring force in the  $x$  and  $y$  coordinates, and a cubic anharmonic coupling term. The Morse fit potential is not accurate for large values of  $\theta$ . The appropriate pairwise functions and parameters are given in Refs. 4 and 23.

A contour plot of the global fit *ab initio* potential is shown in Fig. 2. The empirical and *ab initio* surfaces are qualitatively similar. Both have binding energies of about  $400\text{ cm}^{-1}$  with minimum barriers to internal rotation of approximately half the binding energy. Both potentials are also strongly anisotropic due to the shape of the benzene  $\pi$  orbitals. Along the minimum energy path of the argon in the angular coordinate around benzene, the center-of-mass separation increases from  $3.5\text{ \AA}$  at  $\theta=0$  to  $5.1\text{ \AA}$  at  $\theta=\pi/2$ . The center-of-mass separation also increases more rapidly near the equilibrium configuration.

The strong potential anisotropy highlights a significant disadvantage of angular momentum basis sets—the need to expand the potential in angular functions. When the barriers to rotation are high, a large number of terms are needed to converge the expansion and for each new potential additional care must be taken to see that convergence is obtained. Brocks and Huygen, for example, needed spherical harmonics up to  $l_{\text{max}}=36$  for their calculations on Ar–benzene.<sup>4</sup> Localized basis sets are more flexible because they do not rely on expansion in a particular functional form.

Determination of the expansion coefficients by numerical quadratures is also complicated by singularities arising from the 6–12 form of the potentials. The problem arises from the fact that in a direct-product expansion with delocalized functions the basis functions may have significant amplitude near the singularities, and the integrals become extremely sensitive to the choice of quadrature points. These singularities may pose difficulties even for quadratures over the localized Gaussian basis functions used in this work. For this reason, it is desirable to fit the individual pair potentials to a nonsingular functional form for regions near the atomic nuclei. The method employed here is to fit each pair potential to the functional form

$$v_q(r) = A_q e^{-b_q r}, \quad r < r_{\text{cutoff}}, \quad (9)$$

where  $q$  represents either C or H and the coefficients  $A_q$  and  $b_q$  are chosen to preserve the continuity of the pair potential and its derivative at  $r_{\text{cutoff}}$ . Provided that  $r_{\text{cutoff}}$  is chosen reasonably small, this damping should not have any physical consequence at the energies in which we are interested. For this work a choice of  $r_{\text{cutoff}}=1.0\text{ \AA}$  was found to be adequate, and the associated parameters for the two potentials are shown in Table I. Varying the choice of  $r_{\text{cutoff}}$  was found to have no effect on the eigenenergies to at least 11 significant digits.

Given the relatively large reduced mass of the complex and small rotational constant of the benzene (corresponding to a large reduced bending mass), one expects that in the low-lying vibrational states the argon will be localized on one side of the benzene molecule. The vdW vibrational states may thus be classified in the reduced symmetry group  $C_{6v}$  rather than the full symmetry group of the potential,  $D_{6h}$ .<sup>4</sup> The vdW stretch belongs to the totally symmetric representation  $A_1$ , while the bend belongs to the representation  $E_1$ . The symmetry of the overtones and combinations can be determined in the standard ways.<sup>26</sup>

TABLE I. Potential and geometric data for Ar-benzene.

	Empirical <sup>a</sup>	Global Fit <sup>b</sup>	Morse Fit <sup>c</sup>
Molecular geometry <sup>d</sup>			
C-H(Å)	1.084	1.080	...
C-C(Å)	1.395	1.406	...
Rotation constants			
A(cm <sup>-1</sup> )	0.189 754	0.189 754	0.189 754
C(cm <sup>-1</sup> )	0.094 877	0.094 877	0.094 877
Potential minimum			
D <sub>e</sub> (cm <sup>-1</sup> )	352.56	393.46	425.00
z <sub>e</sub> (Å)	3.494	3.555	3.553
Rot. barrier(cm <sup>-1</sup> )	196.1	228.3	...
Additional parameters <sup>e</sup>			
r <sub>cutoff</sub> (Å)	1.0	1.0	...
A <sub>C</sub> (cm <sup>-1</sup> )	6.7×10 <sup>13</sup>	1.7×10 <sup>15</sup>	...
A <sub>H</sub> (cm <sup>-1</sup> )	2.6×10 <sup>13</sup>	4.6×10 <sup>13</sup>	...
b <sub>C</sub> (Å <sup>-1</sup> )	12.0	13.3	...
b <sub>H</sub> (Å <sup>-1</sup> )	12.0	13.2	...

<sup>a</sup>Parameters from Ref. 4.<sup>b</sup>Parameters from global fit A of Ref. 23.<sup>c</sup>Parameters from Ref. 23.<sup>d</sup>Used in calculation of potential only.<sup>e</sup>See Eq. (9).

#### D. Basis set

The solution to the Schrödinger equation for this Hamiltonian may be expanded as

$$\psi = \frac{1}{R} \sum_{i,j,k} c_{ijk} f_i(R) \phi_{jk}(\theta, \chi), \quad (10)$$

where the sets of  $f_i$  and  $\phi_{jk}$  represent complete bases in their respective coordinates.

Approximate variational solutions may be obtained by simply taking subsets of the complete basis appropriate to a given range of energies (in this case the energies of the lowest lying bound states). For example, in many atom-diatom complexes it is appropriate to use a relatively localized set of Gaussians in the radial coordinate because the stretching motion is fairly stiff. The angular motion in these complexes is often nearly that of a free rotor, so a fairly small set of spherical harmonics may be used. The angular motion in argon-benzene, however, is quite constrained in the angular coordinate  $\theta$ , and a very large basis of angular momentum functions must be used to converge even the lowest eigenstates.<sup>4</sup>

A reasonable solution to this problem is to choose localized bases for *all* of the coordinates for which motion on the potential surface is localized. This solution also avoids the difficulty of a slowly converging potential expansion, because no functional form of the potential is assumed in the localized coordinates. For the argon-benzene complex, the basis should be localized in the  $R$  and  $\theta$  coordinates, but not in the  $\chi$  coordinate. Because of the six-fold symmetry, the potential may be expanded

$$V(R, \theta, \chi) \equiv V_0(R, \theta) + V_6(R, \theta) \cos 6\chi + \dots \quad (11)$$

Thus, if the basis functions in the  $\chi$  coordinate are taken to be eigenfunctions of one-dimensional rotation,  $e^{\pm ik\chi}$ , the Hamiltonian will only couple states with the selection rule  $\Delta k = 0 \pmod 6$ . To first order the  $V_6$  term may be neglected because the center-of-mass separation is relatively large compared to the atomic dimensions. Calculation of the low-lying vibrational states may then be carried out with the assumption that states of different  $k$  are not coupled, effectively reducing the dimensionality of the problem. The first-order Hamiltonian is thus block-diagonal in  $k$ . The first-order eigenstates obtained from these calculations may then be used as a basis for a fully coupled calculation. For the majority of low-lying states, however, this coupling proves to be negligible given the accuracy to which the potential is known, and should have only a very small effect.

The basis chosen for this problem is thus a direct product of Gaussians in  $R$  and  $\theta$  distributed on a rectangular grid, with the appropriate near eigenfunctions of rotation in the  $\chi$  coordinate. The components of this basis are given by

$$f_i(R) = \exp[-A_i^R (R - R_i)^2], \quad (12)$$

$$\begin{aligned} \phi_{jk}(\theta, \chi) = & \exp[-A_j^\theta (\theta - \theta_j)^2] \\ & \times \sin^k \theta \begin{cases} \cos k \chi, & + \text{parity} \\ \sin k \chi, & - \text{parity} \end{cases} \end{aligned} \quad (13)$$

where the  $R_i$  and  $\theta_j$  are the positions of the Gaussian centers, and  $k$  is the unsigned azimuthal quantum number corresponding to rotation of the benzene about its symmetry axis. The sign of  $k$  is replaced by the parity quantum number,  $p = \pm 1$ , which is rigorously conserved. The selection rule for the coupling of different  $k$  states by the potential becomes

$$k' \pm k'' = 0 \pmod 6. \quad (14)$$

For  $k=0$ , only the  $+1$  parity state exists. Normalization is taken into account in the overlap matrix. The extra  $\sin^k \theta$  term in the angular basis function is added to produce the correct asymptotic behavior at the singular point  $\theta=0$ . Without the addition of this term, singularities arise in  $k \neq 0$  matrix elements of the kinetic energy.

For equally spaced Gaussians the preexponential factors may be chosen by Hamilton and Light's formula<sup>14</sup>

$$A_R = C_R^2 / \Delta_R^2, \quad A_\theta = C_\theta^2 / \Delta_\theta^2 \quad (15)$$

where the  $\Delta$ 's are the grid spacing and the  $C$ 's are width parameters which may be chosen to optimize the performance of the basis. Choices of width parameter outside the range 0.4 to 1.4 can lead to problems with linear dependence on one end and slow convergence on the other. It is useful for a given problem to optimize the width parameter for each coordinate in a separate one- or two-dimensional calculation, as is done here. For these calculations the values  $C_R = 1.0$  and  $C_\theta = 0.4$  were found to be nearly optimal and are used throughout.

TABLE II. Symmetry species of  $J=0$  basis functions.

$k \bmod 6$	parity	$\Gamma(C_{6v})$
0	+	$A_1$
0	-	$A_2$
1,5	+/-	$E_1$
2,4	+/-	$E_2$
3	+	$B_2$
3	-	$B_1$

Because the Gaussians form a nonorthogonal basis, the variational solutions are obtained by solving the generalized eigenvalue problem

$$(\mathbf{H} - E_n \mathbf{S}) \mathbf{u}_n = 0, \quad (16)$$

where  $\mathbf{H}$  is the Hamiltonian matrix,  $\mathbf{S}$  is the overlap matrix, and the solutions  $E_n$  and  $\mathbf{u}_n$  are the variational eigenenergies and eigenfunctions, respectively. The solutions are found numerically using a subroutine from the NAG Fortran library.<sup>27</sup>

The basis functions may be classified according to the point group  $C_{6v}$  for the purpose of labeling the eigenstates and block factoring the Hamiltonian matrix. Basis functions of different overall symmetry will have no coupling matrix elements between them. A detailed symmetry analysis is given in Ref. 4, however, the symmetry labels may be determined for the  $J=0$  case in a straightforward manner from the effect of the point group operations on the primitive basis functions. Since the point group operations do not affect the  $R$  and  $\theta$  coordinates, the labels depend on  $k$  and  $p$  alone. The appropriate symmetry labels are shown in Table II. For the states of  $E$  symmetry, calculation of a single parity component is sufficient.

The eigenstates are also labeled in the conventional spectroscopic notation,  $v_b^l v_s$ , where  $v_b$  is the number of bend quanta in the vdW bend,  $l$  is the vibrational angular momentum of the vdW bend, and  $v_s$  is the number of vdW stretch quanta. For the  $J=0$  Hamiltonian, the vibrational angular momentum is  $k$ , as suggested by the symmetry classification of the basis states. Because of the selection rule in Eq. (14) the  $k$  quantum number is nearly conserved and is a good label for all of the states discussed here, while the  $v_s$  and  $v_b$  labels break down when there are strong bend-stretch interactions. A reasonably straightforward extension of the basis set to nonzero  $J$  is presented in the Appendix.

## E. Full calculations

The basis set for the three-dimensional calculations consists of a rectangular grid of Gaussians in  $R$  and  $\theta$  for each value of  $p$  and for  $k$  below the cutoff  $k_{\max}$ . Only states of one  $p$  value need to be calculated for each of the two degenerate representations, since  $p$  is a rigorously conserved quantum number. To reduce the size of the matrix diagonalizations that must be performed, the blocks in each  $k$  quantum number within each symmetry block of the Hamiltonian are diagonalized first. The resulting states are near eigenstates of the full Hamiltonian coupled only

by weak potential terms and the selection rule of Eq. (14). Because  $k$  represents the minimum number of vibrational quanta, the states of different  $k$  that can couple should be well-separated in energy, at least for the states of only a few quanta of excitation that are of interest here. The energies of these states should thus be a good approximation to the exact eigenenergies. These  $k$ -uncoupled states are then used to form a basis of greatly reduced size for the full Hamiltonian. Only states below the energy  $V_{\text{cutoff}}$  are included. This contraction parameter is chosen to lie well outside the energy range of interest. The resulting matrix is then diagonalized to give the fully coupled eigenstates.

The size of this basis set may be reduced further by removing elements centered at points where the potential is greater than some cutoff value,  $V_{\max}$ . This method was suggested by Peet<sup>15</sup> and provides a simple way to construct an efficient nondirect product basis. For this problem the value of the potential at  $(R_i, \theta_j, 0)$  is used to determine whether a given basis function is discarded.

The overlap and kinetic energy matrix elements may be written as the products of one-dimensional integrals. The radial components have analytic factors which are given elsewhere<sup>14</sup> or may be simply derived. The angular integrals may be computed by simple numerical quadratures and are diagonal in the quantum number  $k$ . Computation of these matrices is thus very efficient, accounting for less than 1% of the total computational time.

The potential matrix elements are not separable and must be evaluated in the full three-dimensional space. Multidimensional numerical quadrature is considerably more costly, and the evaluation of these integrals consumes between 50% and 80% of the computational time for the basis sizes considered here. The remainder of the time is spent on the diagonalization. For larger basis sets, the diagonalization time becomes rapidly dominant because the operation goes as  $N^3$ , whereas evaluating the matrix elements is of order  $N^2$  or  $N$ .

One technical point worthy of note is the efficiency of rectangular grid spacing. Integrals over products of equal-width Gaussians reduce conveniently to integrals over a single Gaussian centered at the mean position, i.e.,

$$\int dR e^{-A(R-R_i)^2} e^{-A(R-R_j)^2} f(R) = e^{-\frac{A}{2}(R_i-R_j)^2} \int dR e^{-2A(R-(R_i+R_j)/2)^2} f(R). \quad (17)$$

Thus, the number of integrals that must be calculated can be reduced from  $\approx N_{\text{gauss}}^2/2$  to  $\approx 4N_{\text{gauss}}$  because the integrals depend only on the distance between the Gaussian centers in each coordinate. For 200 Gaussians, a typical number, this results in a 25-fold savings.

## F. Adiabatic calculations

To elucidate the nature of the bend-stretch interactions calculations are performed with the bend and stretch coordinates adiabatically decoupled. The scheme used here has been called the "reversed-adiabatic approximation,"<sup>28</sup> because  $R$  is taken as the "fast" coordinate. A similar

TABLE III. Basis set parameters for Ar–benzene calculations. The columns are labeled by the estimated accuracy of the first 11 eigenenergies. The third column shows the parameters used to estimate the level of convergence.

parameter	Estimated Convergence		
	0.01 cm <sup>-1</sup>	0.001 cm <sup>-1</sup>	Calibration
<b>Basis size</b>			
$N_R$	15	24	30
$N_\theta$	15	24	30
$N_{\text{tot}}$	183	387	607
$k_{\text{max}}$	6	6	6
<b>Width parameters</b>			
$C_R$	1.0	1.0	1.0
$C_\theta$	0.4	0.4	0.4
<b>Grid</b>			
$R_{\text{min}}$ (Å)	3.1	3.1	3.1
$R_{\text{max}}$ (Å)	5.0	5.0	5.0
$\theta_{\text{max}}$	45°	63°	63°
<b>Potential cutoff</b>			
$V_{\text{max}}$ (cm <sup>-1</sup> )	100.0	100.0	100.0
<b>Basis contraction</b>			
$V_{\text{cutoff}}$ (cm <sup>-1</sup> )	-150.0	-150.0	-100.0

procedure has been employed by Tiller and Clary<sup>9</sup> to investigate bend–stretch coupling in other vdW clusters. The radial Hamiltonian,

$$H_R = -\frac{\hbar^2}{2\mu R} \frac{\partial^2}{\partial R^2} R + V_{\theta,\chi}(R), \quad (18)$$

is solved on a grid of points in  $\theta$  and  $\chi$  using the radial part of the basis described above. The eigenvalues of this Hamiltonian at each point in the angular configuration space determine an effective bending potential, which is a function of the number of stretch quanta. The bend Hamiltonian is thus

$$H_{\text{bend}} = -\left[ \frac{\hbar^2}{2\mu R^2} + A \right] \left( \frac{1}{\sin \theta} \frac{\partial}{\partial \theta} \left( \sin \theta \frac{\partial}{\partial \theta} \right) - \frac{k^2}{\sin^2 \theta} \right) - (A - C) k^2 + V_{\text{bend}}^{v_s}(\theta, \chi). \quad (19)$$

This Hamiltonian is diagonalized, holding  $R$  fixed at the equilibrium value, in the angular basis previously described. The resulting eigenvalues aid in determining the approximate assignment of the exact eigenstates and mark the presence of strong bend–stretch interactions. The adiabatic eigenstates may also be projected onto the exact eigenstates of the three dimensional Hamiltonian in order to determine numerical coefficients for the bend–stretch coupling.

### III. RESULTS AND DISCUSSION

Tests for accuracy of the quadrature scheme and convergence of the eigenenergies were performed by varying the number of quadrature points and basis functions. Extensive tests were done using the empirical potential, and convergence was checked with calculations on all three potential surfaces. With 387 Gaussian basis functions, contracted from a grid of 24 Gaussians in  $R$  and  $\theta$ , the con-

TABLE IV. Converged eigenenergies of the empirical potential from Ref. 4 for  $J=0$ .

Symmetry ( $C_{6v}$ )	Band origin (cm <sup>-1</sup> )	Vibrational assignment ( $v'_b v_s$ ) <sup>b</sup>	$k$ uncoupling effect <sup>a</sup> (cm <sup>-1</sup> )
$A_1$	0.00 <sup>c</sup>	0 <sup>0</sup> 0	0.0000
$E_1$	21.37	1 <sup>1</sup> 0	0.0003
$A_1$	32.28	2 <sup>0</sup> 0 ↔ 0 <sup>0</sup> 1 <sup>d</sup>	0.0014
$E_2$	41.01	2 <sup>2</sup> 0	0.0025
$A_1$	47.78	0 <sup>0</sup> 1 ↔ 2 <sup>0</sup> 0 <sup>d</sup>	0.0039
$E_1$	49.07	3 <sup>1</sup> 0 ↔ 1 <sup>1</sup> 1 <sup>d</sup>	0.0051
$B_1$	58.72	3 <sup>3</sup> 0	... <sup>e</sup>
$B_2$	59.37	3 <sup>3</sup> 0	... <sup>e</sup>
$A_1$	60.32	4 <sup>0</sup> 0 <sup>f</sup>	0.0179
$E_2$	65.15	4 <sup>2</sup> 0 <sup>f</sup>	0.0340
$E_1$	68.76	1 <sup>1</sup> 1 <sup>f</sup>	0.0255

<sup>a</sup>Approximate energy using  $k$ -uncoupling approximation – exact energy.

<sup>b</sup>Approximate labels in standard spectroscopic notation (see text).

<sup>c</sup> $D_0=308.27$  cm<sup>-1</sup>, zero point energy = 44.29 cm<sup>-1</sup>.

<sup>d</sup>Fermi resonant pair.

<sup>e</sup>Not calculated for these states.

<sup>f</sup>These states involve strong mixing among more than five zeroth-order states. Labels represent states with the largest contributions.

vergence of the first eleven eigenstates was better than 0.001 cm<sup>-1</sup>. This level of convergence was demonstrated by subsequent calculations with 485 (24 × 30) and 607 (30 × 30) basis functions. This check also shows that the first 60 eigenenergies (up to about -170 cm<sup>-1</sup> on the empirical potential) are converged to better than 0.01 cm<sup>-1</sup>, the limitation on the accuracy of the higher states being the cutoff imposed on the extent of the angular basis (approximately 60°) and the basis contraction parameter  $V_{\text{cutoff}}$ .

The calculations with 607 basis functions point out one potential drawback to the use of nonorthogonal basis sets. The eigenenergies of some states actually increase by a few ten-thousandths of a cm<sup>-1</sup> due to the introduction of some linear dependence in the basis. A practical limit on accuracy for these calculations thus seems to be about 0.0001 cm<sup>-1</sup>. It may be possible to overcome this problem by prediagonalizing the overlap matrix and removing the problematic eigenfunctions, i.e., those whose eigenvalues

TABLE V. Converged eigenenergies of the global fit potential from Ref. 23 for  $J=0$ .

Symmetry ( $C_{6v}$ )	Band origin (cm <sup>-1</sup> )	Ref. 12 (cm <sup>-1</sup> )	Difference (cm <sup>-1</sup> )	Vibrational assignment ( $v'_b v_s$ )
$A_1$	0.00 <sup>a</sup>	0.00	0.00	0 <sup>0</sup> 0
$E_1$	25.52	25.52	0.00	1 <sup>1</sup> 0
$A_1$	37.50	37.51	-0.01	0 <sup>0</sup> 1 ↔ 2 <sup>0</sup> 0 <sup>b</sup>
$E_2$	49.10	49.12	-0.02	2 <sup>2</sup> 0
$A_1$	54.86	54.89	-0.03	2 <sup>0</sup> 0 ↔ 0 <sup>0</sup> 1 <sup>b</sup>
$E_1$	58.22	58.27	-0.05	3 <sup>1</sup> 0 ↔ 1 <sup>1</sup> 1 <sup>b</sup>
$B_1$	70.63	70.72	-0.09	3 <sup>3</sup> 0
$A_1$	70.81	71.20	-0.39	4 <sup>0</sup> 0 <sup>c</sup>
$B_2$	71.00	71.08	-0.08	3 <sup>3</sup> 0
$E_2$	77.84	N/A	N/A	4 <sup>2</sup> 0 <sup>c</sup>
$E_1$	79.82	N/A	N/A	1 <sup>1</sup> 1 <sup>c</sup>

<sup>a</sup> $D_0=342.47$  cm<sup>-1</sup>, zero point energy = 50.99 cm<sup>-1</sup>.

<sup>b</sup>Fermi resonant pair.

<sup>c</sup>Mixing involves more than five zeroth-order states.

TABLE VI. Converged eigenenergies of the Morse fit potential from Ref. 23 for  $J=0$  compared with experimental band origins from Ref. 19 and the recent reassignment by Ref. 24.

Symmetry ( $C_{6v}$ )	Calculated		Band type <sup>a</sup>	REMPI Spectrum	
	Band origin ( $\text{cm}^{-1}$ )	Vibrational assignment ( $v_b^i, v_s$ )		Band origin ( $\text{cm}^{-1}$ )	Band type
$A_1$	0.00 <sup>b</sup>	$0^0 0$	perpendicular	0.0	perpendicular
$E_1$	30.17	$1^1 0$	parallel	31.2	parallel
$A_1$	41.02	$0^0 1^c$	perpendicular	40.1	perpendicular
$E_2$	60.34	$2^2 0$	perpendicular		not observed
$A_1$	64.38	$2^0 0^c$	perpendicular	62.9	perpendicular
$E_1$	68.44	$1^1 1^c$	parallel		not observed
$A_1$	79.34	$0^0 2^c$	perpendicular		not observed
$B_2$	90.50	$3^3 0^c$	"forbidden"		not observed
$B_1$	90.50	$3^3 0^c$	"forbidden"		not observed

<sup>a</sup>Based on symmetry considerations (see text).

<sup>b</sup> $D_0=371.48 \text{ cm}^{-1}$ , zero point energy =  $53.52 \text{ cm}^{-1}$ .

<sup>c</sup>Bend-stretch mixing is still present (see Fig. 6), but strong Fermi resonances do not occur for low-lying states.

fall below some very small cutoff. This procedure was not investigated, however, in the present work. For most applications, the accuracy of one part in  $10^6$  or  $10^7$  obtained here would seem sufficient.

Values of some basis set parameters used in the calculations and their resulting levels of convergence are shown in Table III. The third column shows the largest basis set used to estimate convergence. The first set of parameters shown were found to give better than  $0.01 \text{ cm}^{-1}$  accuracy for the first eight eigenstates. Run time for a fully coupled calculation on a DEC Alpha AXP3000 workstation was approximately 200 s. An uncoupled calculation using these parameters on the first two  $k$  levels required only 30 s of CPU time, suggesting that such a procedure could be included inside a least-squares fitting loop if sufficient data were available.

The  $k$ -uncoupling approximation was found to be very accurate for all the states of interest here on all three potential surfaces. The off-diagonal elements of the full Hamiltonian matrix constructed from the uncoupled states were generally smaller than  $0.1 \text{ cm}^{-1}$ . The effect on the resulting eigenstates is thus very small, as one would expect from second-order perturbation theory. The size of this effect is shown in Table IV along with a summary of results on the empirical potential converged to better than  $0.001 \text{ cm}^{-1}$ .

Vibrational assignments are also given in terms of the approximate bend and stretch quantum numbers, with multiple assignments denoting near-resonant pairs. The resonances are discussed below. The eigenenergies as well as the expectation values of geometric parameters from the wave functions obtained are in excellent agreement with those in Table IX of Ref. 4.

Results from the global fit and Morse fit potentials are shown in Tables V and VI. The results shown are again converged to better than  $0.001 \text{ cm}^{-1}$ . There is some unexplained disparity between these results and the calculations of Bludský *et al.*<sup>23</sup> on the same potentials. The differences are on the order of several wavenumbers for the states

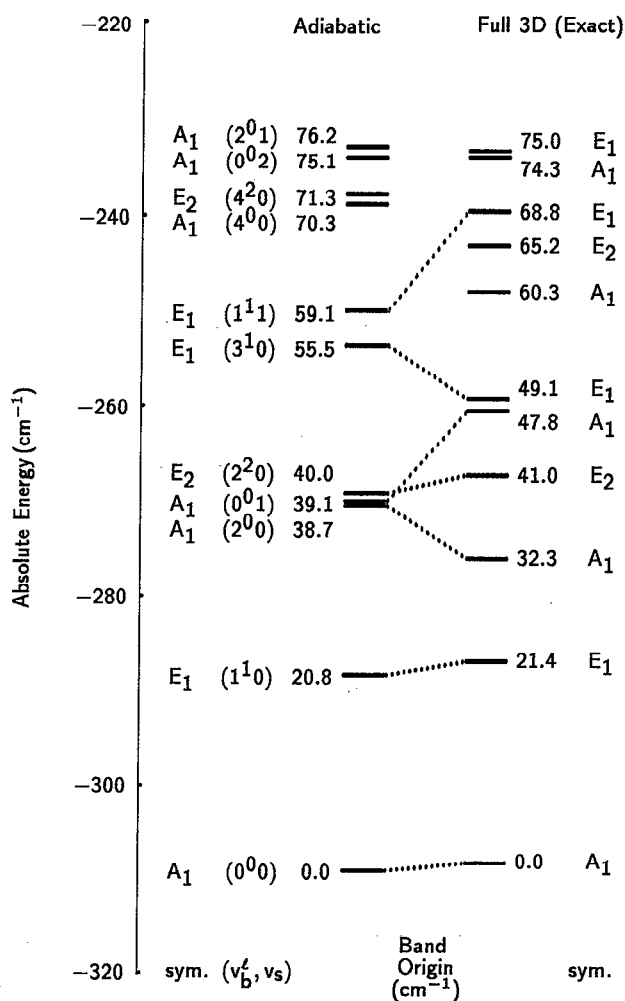


FIG. 3. Correlation diagram for vibrational states on the empirical potential surface from Ref. 4. The zeroth-order states from the adiabatic calculations are correlated with the exact eigenstates of the full three-dimensional Hamiltonian. Strong Fermi-type resonances are observed due to the near 2:1 ratio of zeroth-order stretch and bend frequencies. Only the bend fundamental ( $1^1 0$ ) and the  $E_2$  component of the overtone ( $2^2 0$ ) have nearly conserved bend-stretch quantum numbers. The states of  $B$  symmetry are omitted for the sake of clarity.

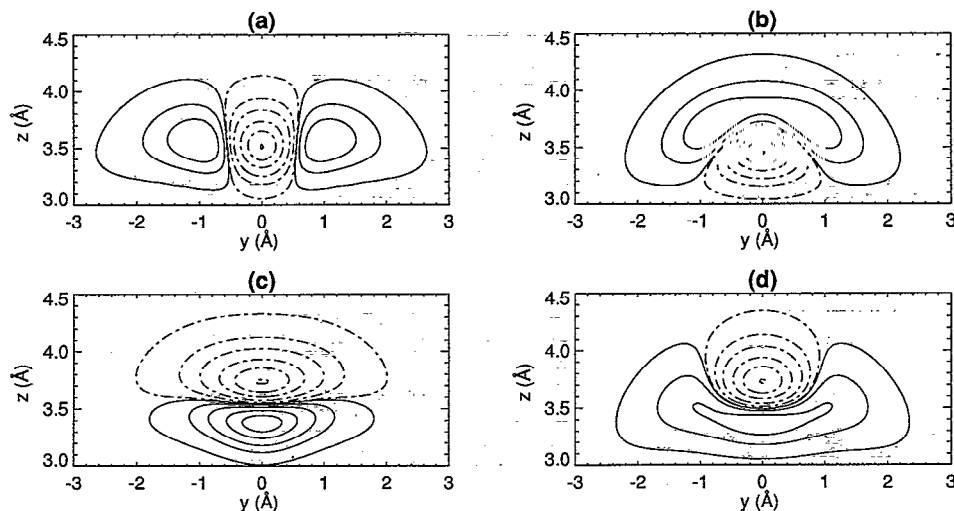


FIG. 4. Fermi-type resonance between the vdW stretch fundamental and the bend overtone on the empirical potential surface of Ref. 4. The zeroth-order states, shown on the left, are calculated using the adiabatic method of Sec. II, which neglects the bend–stretch interaction. State (a) is the adiabatic bend overtone at  $38.7\text{ cm}^{-1}$  and state (c) is the adiabatic stretch fundamental at  $39.1\text{ cm}^{-1}$ . The exact eigenstates (b) and (d), have energies of  $32.3$  and  $47.8\text{ cm}^{-1}$  respectively. Bend–stretch interactions couple the nearly degenerate adiabatic states so that the exact eigenstates are almost 1:1 mixtures of the resonant zeroth-order states.

shown. There is, however, far better agreement with the more recent calculations of van der Avoird.<sup>12</sup> A comparison of the calculated eigenenergies on the global potential is shown in Table V. The only disagreement outside the level of convergence estimated in van der Avoird’s paper—from  $0.01$ – $0.10\text{ cm}^{-1}$  for the first ten states—is for the fourth state of  $A_1$  symmetry. There is a slight difference in the values of the rotation constants which are used, but this cannot account for a  $0.4\text{ cm}^{-1}$  discrepancy. The potential parameters used here have been carefully checked against those of Refs. 12 and 23, so that the direction of the disagreement seems to indicate that the results shown here are better converged. The results on the Morse fit potential are, however, in very good agreement. The eigenenergies differ by at most  $\pm 0.01\text{ cm}^{-1}$ , and the expectation values of the geometric parameters agree to all decimal places reported in Ref. 12. This agreement is strong evidence that both results are essentially correct, since the methods employed are completely different and the calculations were performed independently.

As mentioned above, the Hamiltonian couples zeroth-order bend and stretch states of the same symmetry. In several cases, most notably for states on the empirical potential surface, the coupling matrix elements are larger than the zeroth-order separations, leading to large Fermi-type resonances. The zeroth-order energies determined by the adiabatic calculations enable approximate assignment of these resonant states. Using the adiabatic states as a basis, we can determine the coupling matrix elements and the extent of mixing. These calculations reveal that above the first several vibrational levels on the empirical potential, a large number of the adiabatic states contribute to the exact eigenstates, and the approximate vibrational assignments become meaningless.

A correlation diagram is shown in Fig. 3. The first

prominent resonance occurs between the zeroth-order stretch ( $0^0_1$ ) and the totally symmetric component of the bend overtone ( $2^0_0$ ). The zeroth order states are nearly degenerate with a coupling matrix element of approximately  $8\text{ cm}^{-1}$ . This coupling matrix element can be directly inferred from the correlation diagram if one assumes the dominant interaction occurs only between these two states. The strong mixing of the zeroth-order wave functions in the exact eigenstates can be seen in Fig. 4. For the next group of  $A_1$  states beginning at  $60.3\text{ cm}^{-1}$ , the number of contributing zeroth-order states increases to about seven, completely invalidating the approximate labeling scheme. These results demonstrate the possible pitfalls in attempting to label experimentally observed bands with vibrational mode quantum numbers or in applying simple deperturbation schemes based on two- or three-state models.

The coupling on the empirical potential represents an extreme case, since the two normal mode frequencies are in almost exact 2:1 resonance. However, the same qualitative picture holds on the global fit potential (Fig. 5). Coupling on the Morse fit surface (Fig. 6) is somewhat less pronounced because the bend and stretch frequencies are shifted out of resonance and the form of the potential neglects some of the anharmonic terms. The Morse fit potential is also cylindrically symmetric so that  $k$  is exactly conserved. The effects of mixing are still on the order of several  $\text{cm}^{-1}$ , however, and thus should be included in any attempt to make an accurate comparison between the eigenstates of a given potential and experimental data.

The results from the calculations on the Morse fit potential may be used to aid in the assignment of the experimentally obtained REMPI spectrum. This potential is more relevant than the global fit potential for this comparison because it achieves a better fit to the *ab initio* points in

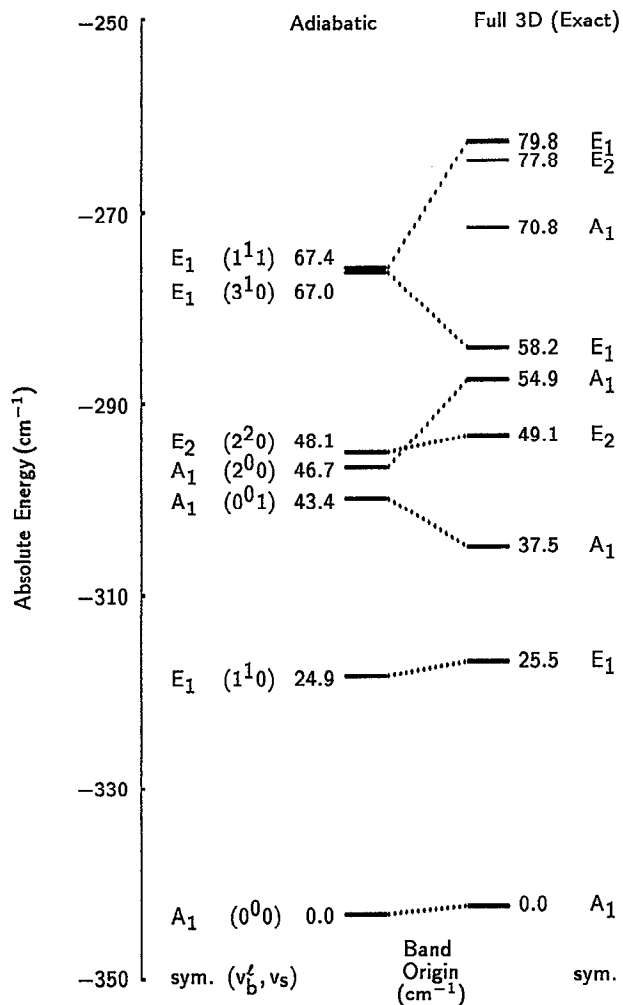


FIG. 5. Correlation diagram for vibrational states on the global fit *ab initio* potential surface from Ref. 23. The zeroth-order states from the adiabatic calculations are correlated with the exact eigenstates of the full three-dimensional Hamiltonian. Fermi-type resonances are still observed although the zeroth-order bend and stretch frequencies have been shifted somewhat out of resonance. Anharmonicity enhances the coupling by decreasing the separation of the adiabatic states. The states of *B* symmetry have been omitted for the sake of clarity.

the region of interest. Only three excited vdW bands have been observed experimentally in the ultraviolet spectrum and there has been some disagreement in the literature<sup>12,17,19,23</sup> over the symmetry and approximate vibrational quantum numbers of the observed states. One caveat is needed in making the comparison between the calculations on the *ab initio* surfaces used here and the experimental results. The experiments probe the intermolecular potential of the benzene's excited  $S_1$  electronic state with the additional excitation of the  $\nu_6$  vibrational mode of benzene to make the UV transition vibronically allowed,<sup>19</sup> whereas the *ab initio* calculations were performed on the ground electronic state of benzene at its equilibrium geometry. The comparison may be justified on the grounds that electronic  $\pi \rightarrow \pi^*$  excitation involves only a slight change in the overall electronic configuration and the expansion of the benzene ring due to the electronic and vibrational excitation is small in comparison to the Ar–benzene bondlength. The

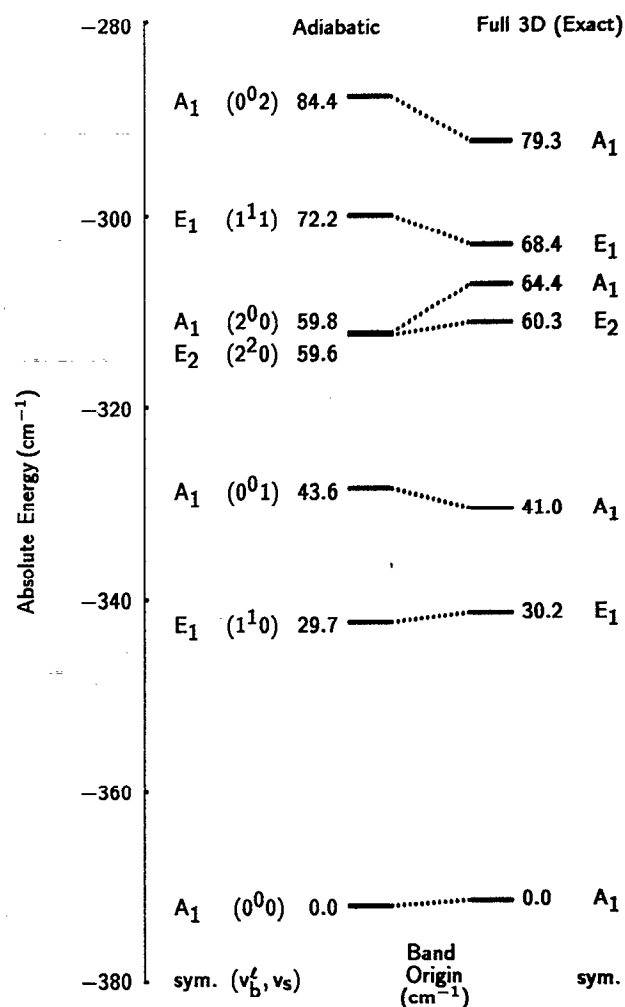


FIG. 6. Correlation diagram for vibrational states on the Morse fit *ab initio* potential surface from Ref. 23. The zeroth-order states from the adiabatic calculations are correlated with the exact eigenstates of the full three-dimensional Hamiltonian. The bend–stretch coupling is evident but less pronounced than on the two previous potential surfaces. The states of *B* symmetry have been omitted for the sake of clarity.

experimental observations that the vibronic excitation is only slightly red-shifted ( $20 \text{ cm}^{-1}$ ) and causes only a slight ( $0.06 \text{ \AA}$ ) contraction of the Ar–benzene bond support these arguments.

In predicting the observed spectrum one must consider the symmetry of the vibronic state and vdW vibration. The analysis is complicated by the fact that both monomer and vdW vibrations can carry angular momentum. The dipole moment operators have the symmetries  $A_1$  and  $E_1$  in the body-fixed frame, corresponding to parallel and perpendicular transitions respectively. The product of the benzene vibronic state and the  $E_1$  bend yields species of  $A_1$ ,  $A_2$ , and  $E_2$  symmetry, the first of which is accessible by a parallel transition from the ground  $A_1$  state. From the Morse fit potential we can thus predict a parallel band to lie at  $30.2 \text{ cm}^{-1}$ . Similarly, the  $A_1$  vdW states are expected to yield perpendicular transitions, which are predicted at  $41.0$  and  $64.4 \text{ cm}^{-1}$ . The  $E_2$  states can also give rise to perpendicular transitions, although these bands may be ex-

pected to have a more complicated structure due to the coupling of the two vibrational angular momenta. Furthermore, one may argue that the bend overtone of  $A_1$  symmetry is more likely to be observed because it may borrow intensity from the stretch fundamental through mixing, which we have seen is a prominent feature of the potential.

On the basis of these observations we may predict that the first three observable bands will be a parallel band due to the bend fundamental, a perpendicular band due to the stretch fundamental, and a second perpendicular band due to the bend overtone of  $A_1$  symmetry, at 30.2, 41.0, and 64.4  $\text{cm}^{-1}$  respectively. The relative intensities of the two perpendicular bands will be sensitive to the degree of mixing through anharmonic coupling. van der Avoird<sup>12</sup> has reached the same conclusion on the basis of similar calculations and analysis. These predictions are in reasonably good agreement with the experimental results. The three experimentally observed bands have been rotationally resolved with origins at 31.5, 40.1, and 62.9  $\text{cm}^{-1}$ .<sup>19,24</sup> The first of these bands has only recently been definitively assigned<sup>24</sup> as a parallel band with the revised origin of 31.2  $\text{cm}^{-1}$ . The previous assignment as the bend overtone ( $2^0$  or  $2^0$ ) could not be reconciled with any of the calculated eigenspectra, particularly since it was known from the rotational structure that the bands at 31 and 40  $\text{cm}^{-1}$  did not correspond to states of the same symmetry. It is interesting to note that this assignment places the bending frequency about 50% higher than that observed in other Ar-aromatic complexes.<sup>22</sup> No explanation for this observation is immediately evident. The two remaining bands have perpendicular structure and have now been assigned as the stretch fundamental and symmetric bend overtone respectively,<sup>24</sup> bringing theory and experiment into agreement.

#### IV. CONCLUSIONS

Many other methods currently exist for calculating vdW spectra with comparable accuracy and computational demands. The recent calculations of van der Avoird<sup>12</sup> and of Mandziuk and Bačić<sup>10</sup> are just two examples. The use of Gaussians has the advantages of simplicity and flexibility. It is always easy to construct an efficient basis of Gaussian functions which avoids non-physical regions of the potential. The method is assured of being accurate and relatively straightforward to implement.

A three-dimensional basis of angular and radial Gaussians combined with monomer azimuthal rotation functions has been shown to be highly efficient for the calculation of Ar-benzene vdW states. For the strongly anisotropic potentials considered here, the low-lying vibrational states were accurately obtained when the angular range of the basis was sharply restricted. The  $k$ -uncoupling approximation, which one would expect to hold for other atom-symmetric top complexes, allows accurate and extremely rapid calculation of the lowest-lying vibrational states for comparison with experimentally observed bands.

The extension of the basis to nonzero  $J$  described in the Appendix also holds promise for the efficient prediction of high-resolution rovibrational spectra.

The eigenstates of the empirical potential show a high degree of bend-stretch mixing which completely alters the resulting eigenspectrum. This mixing can be understood in terms of a near-exact 2:1 resonance between the bend and stretch frequencies, as revealed by the adiabatic calculations. The effect of this coupling is diminished in the spectra predicted from the *ab initio* surfaces as the bend and stretch frequencies are brought out of resonance, though the coupling remains strong enough to shift the levels significantly. Given the ease with which the full three-dimensional calculations can now be performed, it would seem unwise to use approximate methods when predicting vibrational spectra from model potential surfaces when such coupling may be in effect.

Comparison of the results from the Morse fit potential with the recently reassigned experimental bands<sup>24</sup> shows considerably better agreement than has been previously attained. It is worthy of note that these eigenvalues are obtained without reference to experimental information on the vdW interactions. The combination of high level electronic structure and vibrational quantum calculations may thus be valuable in predicting and understanding spectra of aromatic and other larger vdW clusters.

#### ACKNOWLEDGMENTS

I would like to thank David Nesbitt, Eberhard Riedle, and Robert Parson for their assistance and encouragement in the completion of this work. I would also like to thank Paul Maslen, and Jeremy Hutson for their careful readings of this manuscript and helpful suggestions. Finally, I thank the National Science Foundation for the award of a Graduate Fellowship.

#### APPENDIX: $J \neq 0$ BASIS SET

Calculations at nonzero  $J$  yield important information about rotational structure and the Coriolis interactions that mix vibrational states. In the past these calculations have been very expensive to perform, but van der Avoird<sup>12</sup> has recently obtained  $J \neq 0$  results relatively easily using a three-dimensional harmonic oscillator basis set. Extension of the present method should also allow computation of the  $J \neq 0$  states at a very modest increase in the computational cost once the expensive potential matrix elements have been evaluated in a  $J=0$  calculation.

Construction of the nonzero  $J$  basis functions is straightforward. A key aspect of the construction is that the  $J=0$  Gaussians in  $R$  and  $\theta$  are retained, which will eliminate the need to evaluate any more multidimensional integrals. The generalized basis functions are taken to be linear combinations of eigenfunctions of the total angular momentum  $J$ , its space-fixed projection  $M$ , and its body-fixed projection  $K$ . Recall that the  $\phi$  angle represents rotation of the molecular axis system about the body-fixed

axis  $R$ . Motion in this angle thus represents the projection of the total angular momentum onto the body-fixed axis. The exact form of the rotational part of the basis functions is dictated by the two-angle embedding scheme used to derive Eq. (2).<sup>25,28</sup> For clarity I will write the part of the wavefunction on which  $\hat{J}$  operates in the bra and ket notation using a symmetric top representation, and I will write the part of the wavefunction on which  $\hat{j}$  operates in the coordinate representation. The remainder of the wavefunction involves the familiar Gaussians in  $R$  and  $\theta$ . The basis functions are then

$$\begin{aligned} \langle \phi\chi | JMKkpij \rangle = & N_{Kk} [ |JKM\rangle e^{iK\phi} e^{ik\chi} \\ & + (-1)^{K+J} |J-KM\rangle e^{-iK\phi} e^{-ik\chi} ] \\ & \times |i\rangle |jKk\rangle, \end{aligned} \quad (\text{A1})$$

where

$$\langle R | i \rangle = \exp[-A_i^R (R - R_i)^2] / R$$

and

$$\langle \theta | jKk \rangle = \sin^{|K-k|} \theta \exp[-A_j^\theta (\theta - \theta_j)^2].$$

$K$  is a signed integer running from  $-J$  to  $J$  and  $k$  is unsigned. The normalization factor  $N_{Kk}$  is added to normalize the bracketed portion of the basis function. The parity quantum number  $p$  takes the values  $\pm 1$  and is consistent with the earlier definition for  $J=0$ . As before, the parity is rigorously conserved, meaning that for states belonging to a degenerate representation, only one  $p$  component must be calculated. The effective vibrational angular momentum quantum number is now  $l = |K - k|$ . From the symmetry analysis in Tables II and IV of Ref. 4, it can be seen that only the subscripts of the nondegenerate representations are affected by the rotational portion of the basis functions. The basis set of Eq. (A1) has been constructed so that the symmetry classifications of Table II here remain valid for  $J \neq 0$ .

The Hamiltonian of Eq. (5) must now be modified by the addition of several terms. The square of the body-fixed angular momentum becomes<sup>29</sup>

$$\begin{aligned} \hat{j}^2 = & \frac{1}{\sin \theta} \frac{\partial}{\partial \theta} \left( \sin \theta \frac{\partial}{\partial \theta} \right) - \frac{1}{\sin^2 \theta} \\ & \times \left( \frac{\partial^2}{\partial \phi^2} + \frac{\partial^2}{\partial \chi^2} - 2 \cos \theta \frac{\partial^2}{\partial \phi \partial \chi} \right). \end{aligned} \quad (\text{A2})$$

This modified operator introduces no new coupling, i.e. it is diagonal in all of the quantum numbers except the indices of the Gaussians. Evaluation of the matrix elements thus requires only an additional term in the one-dimensional integration over  $\theta$ . The remaining terms arise from the dot product in Eq. (2)

$$-2\hat{j} \cdot \hat{J} = -2\hat{j}_Z \hat{J}_Z - \hat{j}_+ \hat{J}_+ - \hat{j}_- \hat{J}_-, \quad (\text{A3})$$

where  $Z$  denotes the body-fixed axis and the operators have the meanings

$$\hat{j}_Z = -i \frac{\partial}{\partial \phi},$$

$$\hat{j}_Z |JKM\rangle = K |JKM\rangle,$$

$$\hat{j}_\pm = -ie^{\pm i\phi} \left[ -\cot \theta \frac{\partial}{\partial \phi} + \frac{1}{\sin \theta} \frac{\partial}{\partial \chi} \pm i \frac{\partial}{\partial \theta} \right],$$

$$\langle J'K'M' | \hat{j}_\pm |JKM\rangle$$

$$= [J(J+1) - K(K \pm 1)]^{1/2} \delta_{JJ'} \delta_{MM'} \delta_{K', K \pm 1}.$$

Note that the sign convention used for  $\hat{j}_\pm$  is opposite to the one used in Zare's book.<sup>29</sup> The  $\hat{j}_Z \hat{J}_Z$  term is diagonal in  $K$ , so the only new coupling arises from the term  $-\hbar^2 (\hat{j}_+ \hat{J}_+ + \hat{j}_- \hat{J}_-) / 2\mu R^2$  in the Hamiltonian, which we may identify as the Coriolis operator. The matrix elements are

$$\begin{aligned} \langle J'K'M'k'p'i'j' | H_{\text{Cor}} | JKMkpij \rangle = & \delta_{JJ'} \delta_{MM'} \delta_{kk'} \delta_{pp'} N_{Kk} N_{K'k'} \langle i' | \frac{\hbar^2}{2\mu R^2} | i \rangle \\ & \times \left\{ \delta_{K', K+1} [J(J+1) - K(K+1)]^{1/2} \langle j'K'k' | -K \cot \theta + \frac{k}{\sin \theta} + \frac{\partial}{\partial \theta} | jKk \rangle \right. \\ & + \delta_{K', K-1} [J(J+1) - K(K-1)]^{1/2} \langle j'K'k' | -K \cot \theta + \frac{k}{\sin \theta} \\ & \left. - \frac{\partial}{\partial \theta} | jKk \rangle \right\}. \end{aligned} \quad (\text{A4})$$

The matrix elements are thus products of algebraic quantities and one dimensional integrals over Gaussian functions, and are not time-consuming to calculate. The Coriolis term will couple states differing by one in  $K$ , but will not mix states of different parity or  $k$ . It will, however, mix states of different  $l$ , giving rise to the commonly known phenomenon of rotational  $l$ -type doubling and other more complicated effects.

The potential matrix elements are given by

$$\begin{aligned}
\langle J'K'M'k'p'i'j' | V(R, \theta, \chi) | JK M k p i j \rangle &= \delta_{JJ'} \delta_{MM'} \delta_{pp'} N_{Kk} N_{K'k'} \\
&\times \{ \delta_{KK'} \langle i'j'Kk' | V(R, \theta, \chi) \cos(k-k') \chi | ijKk \rangle \\
&+ (-1)^{K+J} p \delta_{K',-K} \langle i'j'-Kk' | V(R, \theta, \chi) \cos(k+k') \chi | ijKk \rangle \}.
\end{aligned}
\tag{A5}$$

The second term should be dropped when  $k=0$ . The bracketed quantities on the right hand side are now three dimensional integrals over the potential and the Gaussian functions in  $R$  and  $\theta$ . The symmetry of the potential again yields the coupling selection rule of Eq. (14) for  $k$  and  $k'$ . States of opposite sign in  $K$  are coupled by the  $V_6$  and higher order terms in the potential. It may easily be shown that the potential only couples the effective vibrational angular momentum according the selection rule

$$l \pm l' = 0 \pmod{6}. \tag{A6}$$

Since the integrals in Eq. (A5) depend only on  $l$  and  $l'$ , it is also easy to show from this selection rule that they are the same integrals required for the  $J=0$  calculation.

The method of attacking the  $J \neq 0$  calculations is now easy to see. A  $J=0$  calculation is performed and the potential integrals and eigenstates are stored for use in the nonzero  $J$  calculations. For the basis states of each symmetry, the matrix elements of the kinetic energy operator are evaluated as discussed above. Because each matrix element involves only algebraic factors and one dimensional integrals, the evaluation of the kinetic energy matrix is very fast. The full Hamiltonian matrix is then constructed by the addition of the appropriate  $J=0$  potential matrix elements. The  $J=0$  eigenstates may now be used as a basis to contract the full Hamiltonian matrix. The appropriate  $J=0$  states to use in the contraction are those that have the same  $l$  quantum number. Thus to contract the  $\{J=1, K=-1, k=1\}$  basis states, one would use the  $\{J=0, K=0, k=2\}$  eigenfunctions. The resulting Hamiltonian matrix will be nearly diagonal when the Coriolis terms are small, as one expects for low  $J$ , so the size of the contracted basis may also be relatively small. The time required for such a "truncation and diagonalization" procedure would again be small compared with the time required to compute the potential matrix elements.

Given the minimal computational demands of the method outlined above, nonzero  $J$  calculations should require relatively little time above that required for a  $J=0$

calculation. No three dimensional integration would be required, and no large matrices would need to be diagonalized.

- <sup>1</sup>R.C. Cohen and R.J. Saykally, *J. Phys. Chem.* **94**, 7991 (1990).
- <sup>2</sup>J.M. Hutson, *J. Chem. Phys.* **96**, 6752 (1992).
- <sup>3</sup>J.M. Hutson, *J. Chem. Phys.* **96**, 4237 (1992).
- <sup>4</sup>G. Brocks and T. Huygen, *J. Chem. Phys.* **85**, 3411 (1986).
- <sup>5</sup>G. Brocks and D. van Koeven, *Mol. Phys.* **63**, 999 (1988).
- <sup>6</sup>J.M. Hutson, in *Advances in Molecular Vibrations and Collision Dynamics*, Vol. 1A (JAI, Greenwich, 1991), pp. 1-45.
- <sup>7</sup>W. Yang and A.C. Peet, *J. Phys. Chem.* **153**, 98 (1988); A.C. Peet and W. Yang, *J. Chem. Phys.* **90**, 1746 (1989); *ibid.* **91**, 6598 (1989).
- <sup>8</sup>R.C. Cohen and R.J. Saykally, *Ann. Rev. Phys. Chem.* **42**, 369 (1991).
- <sup>9</sup>A.R. Tiller and D.C. Clary, *Chem. Phys.* **139**, 67 (1989).
- <sup>10</sup>M. Mandziuk and Z. Bačić, *J. Chem. Phys.* **98**, 7165 (1993).
- <sup>11</sup>Z. Bačić and J.C. Light, *J. Chem. Phys.* **85**, 4594 (1986); *Ann. Rev. Phys. Chem.* **40**, 469 (1989); M. Mladenović and Z. Bačić, *J. Chem. Phys.* **94**, 4988 (1991).
- <sup>12</sup>A. van der Avoird, *J. Chem. Phys.* **98**, 5327 (1993).
- <sup>13</sup>J.V. Lill, G.A. Parker, and J.C. Light, *Chem. Phys. Lett.* **89**, 483 (1982); J.C. Light, I.P. Hamilton, and J.V. Lill, *J. Chem. Phys.* **82**, 1400 (1985).
- <sup>14</sup>I.P. Hamilton and J.C. Light, *J. Chem. Phys.* **84**, 306 (1986).
- <sup>15</sup>A.C. Peet, *J. Chem. Phys.* **90**, 4363 (1989).
- <sup>16</sup>Th. Brupbacher and A. Bauder, *Chem. Phys. Lett.* **173**, 435 (1990).
- <sup>17</sup>J.A. Menapace and E.R. Bernstein, *J. Phys. Chem.* **91**, 2533 (1987).
- <sup>18</sup>Th. Weber, A. Bargaen, E. Riedle, and H.J. Neusser, *J. Chem. Phys.* **92**, 90 (1990).
- <sup>19</sup>Th. Weber, thesis, Institut für Physikalische und Theoretische Chemie, Technische Universität München, 1991.
- <sup>20</sup>P. Hobza, H.L. Selze, and E.W. Schlag, *J. Chem. Phys.* **95**, 391 (1991).
- <sup>21</sup>M. Mons and J. Le Calvé, *Chem. Phys.* **146**, 195 (1990).
- <sup>22</sup>E.J. Bieske, M.W. Rainbird, I.M. Atkinson, and A.E. Knight, *J. Chem. Phys.* **9**, 752 (1989).
- <sup>23</sup>O. Bludský, V. Špirko, V. Hrouda, and P. Hobza, *Chem. Phys. Lett.* **196**, 410 (1992).
- <sup>24</sup>E. Riedle (private communication).
- <sup>25</sup>G. Brocks, A. van der Avoird, B.T. Sutcliffe, and J. Tennyson, *Mol. Phys.* **50**, 1025 (1983).
- <sup>26</sup>E.B. Wilson, J.C. Decius, and P.C. Cross, *Molecular Vibrations* (McGraw-Hill, New York, 1955).
- <sup>27</sup>Numerical Algorithms Group routines were used both for the symmetric eigenvalue problem and the various numerical quadrature schemes used to evaluate matrix elements.
- <sup>28</sup>J.M. Hutson, *J. Chem. Phys.* **92**, 157 (1990).
- <sup>29</sup>R.N. Zare, *Angular Momentum* (Wiley-Interscience, New York, 1988), p. 82.